doi:10.1093/jmcb/mjx013
Published online April 28, 2017

Article

Chromodomain protein CDYL is required for transmission/restoration of repressive histone marks

Yongqing Liu[1], Shumeng Liu[1], Shuai Yuan[1], Huajing Yu[1], Yu Zhang[1], Xiaohan Yang[1], Guojia Xie[1], Zhe Chen[1], Wanjin Li[1], Bosen Xu[1], Luyang Sun[1], Yongfeng Shang[1,2,3], and Jing Liang[1,*]

[1] Key Laboratory of Carcinogenesis and Translational Research (Ministry of Education), Department of Biochemistry and Molecular Biology, School of Basic Medical Sciences, Peking University Health Science Center, Beijing 100191, China
[2] Department of Biochemistry and Molecular Biology, School of Basic Medical Sciences, Capital Medical University, Beijing 100069, China
[3] Tianjin Key Laboratory of Medical Epigenetics, Department of Biochemistry and Molecular Biology, School of Basic Medical Sciences, Tianjin Medical University, Tianjin 300070, China
* Correspondence to: Jing Liang, E-mail: liang_jing@hsc.pku.edu.cn

Faithful transmission or restoration of epigenetic information such as repressive histone modifications through generations is critical for the maintenance of cell identity. We report here that chromodomain Y-like protein (CDYL), a chromodomain-containing transcription corepressor, is physically associated with chromatin assembly factor 1 (CAF-1) and the replicative helicase MCM complex. We showed that CDYL bridges CAF-1 and MCM, facilitating histone transfer and deposition during DNA replication. We demonstrated that CDYL recruits histone-modifying enzymes G9a, SETDB1, and EZH2 to replication forks, leading to the addition of H3K9me2/3 and H3K27me2/3 on newly deposited histone H3. Significantly, depletion of CDYL impedes early S phase progression and sensitizes cells to DNA damage. Our data indicate that CDYL plays an important role in the transmission/restoration of repressive histone marks, thereby preserving the epigenetic landscape for the maintenance of cell identity.

Keywords: epigenetic inheritance, histone modification, CDYL, CAF-1, MCM

Introduction

Epigenetics is defined as 'the inheritance of variation above and beyond changes in the DNA sequence' (Bonasio et al., 2010). While chromatin configurations, such as DNA methylation, histone modifications, and histone variants, have certain degree of plasticity, maintenance of epigenetic stability across generations is essential to preserve distinct gene expression profiles in different cell types. Although evidence suggests that maturation of chromatin states could be a continuous process throughout the cell cycle (Chen et al., 2011; Zee et al., 2012; Alabert et al., 2014), proper re-establishment of chromatin structures and epigenetic modifications during replication is critical to maintain cellular memory across generations (Alabert and Groth, 2012; Hathaway et al., 2012). Chromatin reconstruction during replication mainly includes two aspects: (i) disassembly of pre-existing chromatin/releasing of parental histones ahead of replication forks and (ii) deposition of both recycled and newly synthesized histones onto daughter strands. Disassembly of pre-existing chromatin is accompanied by unwinding duplex DNA, a process catalyzed by the multicomponent DNA helicase complex MCM (Bochman and Schwacha, 2009). Interestingly, the MCM complex can serve as a transient docking site for released parental histones (Groth et al., 2007a). It is important to efficiently recycle parental histones, especially for those with modifications involved in gene silencing and chromatin compaction, because these old histones serve as the 'seed' for the propagation of epigenetic information on daughter strands (Campos et al., 2014). Proper reconstruction of chromatin is also dependent on histone chaperones, among which chromatin assembly factor 1 (CAF-1), an evolutionally conserved complex composing of three subunits, p150, p60, and p48, has been reported to deposit newly synthesized H3-H4 onto replicating DNA for *de novo* chromatin assembly (Kaufman et al., 1995; Shibahara and Stillman, 1999). Whether and how CAF-1 is involved in deposition of parental nucleosomal histones still needs investigations.

Compared to the more dynamic transcriptional active histone modifications such as acetylation, the inheritance of repressive histone modifications such as methylation of H3K9 and H3K27

Received August 24, 2016. Revised December 29, 2016. Accepted April 2, 2017.

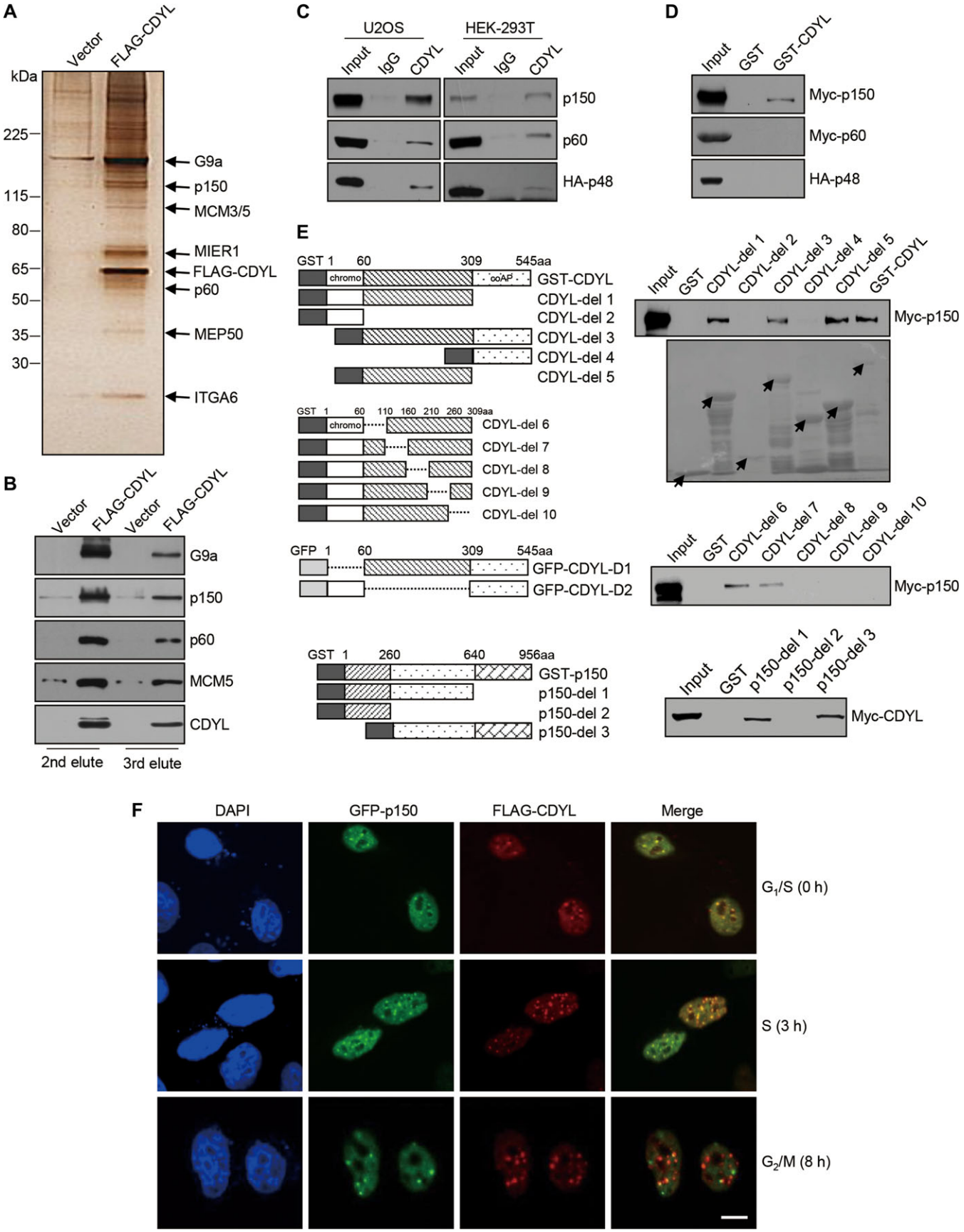

has drawn much attention for their essential roles in proper chromosome segregation, development, and maintenance of cell identity (Whitehouse and Smith, 2013). It is known that H3K9me1/2 are catalyzed by histone methyltransferases (KMTs) G9a/GLP (Tachibana et al., 2005), and H3K9me3 is added by SETDB1 (Schultz et al., 2002) and SUV39H1/2 (O'Carroll et al., 2000; Rea et al., 2000), while H3K27me2/3 are catalyzed by the PRC2 complex, a multisubunit protein assembly containing the catalytic subunit EZH2 and other core constituents SUZ12, EED, and RbAp46/48 (Margueron and Reinberg, 2011). It has been proposed that the EED component of PRC2 specifically binds to H3K27me3-modified histone tails, leading to the propagation of H3K27me3 to neighboring nucleosomes or sister chromatids (Hansen et al., 2008; Margueron et al., 2009). However, the binding affinity of EED for H3K27me3 is significantly lower compared to that of HP1 for H3K9me3 (Vermeulen et al., 2010; Xu et al., 2010), and there is no evidence that EED could be recruited to replication sites where nucleosome reassembly occurs, suggesting other readers exist for efficient transmission of H3K27me3 through cell divisions.

Previously, we reported that the chromodomain Y-like protein (CDYL) exhibits a much stronger affinity toward H3K27me2/3 than EED does. We showed that CDYL directly interacts with EZH2, generating a positive feedback loop to facilitate the propagation of H3K27me3 along chromatin (Zhang et al., 2011). Other researchers have also identified CDYL as one of the strongest binders for H3K27me3 through a genome-wide quantitative interaction proteomics study (Vermeulen et al., 2010). Interestingly, CDYL has been also reported to possess high affinity for H3K9me2/3 (Franz et al., 2009; Bartke et al., 2010; Vermeulen et al., 2010) and interact with G9a (Mulligan et al., 2008). In this study, we investigate the role of CDYL in chromatin reconstruction during replication.

Results

Chromodomain Y-like protein CDYL is physically associated with histone chaperone CAF-1 during S phase

To investigate whether and how CDYL might functionally contribute to the inheritance of the repressive histone modifications, we identified cellular proteins that are associated with CDYL during S phase. In these experiments, FLAG-tagged CDYLb (FLAG-CDYL, we used isoform b, the major CDYL isoform expressed in most human cells) was stably expressed in U2OS cells. Cells were synchronized in G_1/S phase by a double thymidine block and released for 2 h to allow them to enter S phase. Affinity purification using anti-FLAG and mass spectrometry (MS) analysis of the CDYL-containing protein complex revealed that CDYL is associated with multiple proteins including CHAF1a (p150) and CHAF1b (p60), two components of the CAF-1 complex (Figure 1A, the detailed MS results are provided in Supplementary Table S1). This result was confirmed by western blotting with specific antibodies against individual CAF-1 components (Figure 1B). The association between CDYL and CAF-1 *in vivo* was further validated by co-immunoprecipitation (co-IP) assays with antibodies against CDYL followed by immunoblotting (IB) with antibodies against p150, p60, or p48 (Figure 1C). HA-tagged p48 was expressed, because the molecular weight of p48 (48 kDa) is too close to that of the IgG heavy chain (50 kDa). GST pull-down experiments performed with bacterially expressed GST-CDYL and *in vitro* transcribed/translated components of the CAF-1 complex revealed that CDYL interacts directly with p150, but not p60 or p48 (Figure 1D). Further mapping the molecular interface involved in the interaction between CDYL and p150 showed that the region of 161–309 aa in CDYL and the region of 261–640 aa in p150 are responsible for their interaction (Figure 1E), suggesting that the recruitment of the CAF-1 complex by CDYL *in vivo* is through an interaction between CDYL and p150.

To further determine whether the interaction between CDYL and CAF-1 occurs specifically during S phase, we examined the intracellular localization of CDYL and p150 in different phases of the cell cycle. Fluorescent imaging of GFP-p150 and immunostaining of FLAG-CDYL showed that CDYL and p150 were co-localized in the nucleus, but only during G_1/S and S phase; during G_2/M phase, these two proteins were largely apart (Figure 1F). Together, these experiments support the physical association of CDYL and the CAF-1 complex during S phase.

CDYL bridges CAF-1 and chromatin-associated MCM complex

Our affinity purification and MS study also identified MCM3 and MCM5, two components of the MCM complex, interacting with CDYL (Figure 1A). Co-IP assays performed with U2OS cell lysates demonstrated that CDYL indeed interacts with all components of the MCM complex *in vivo* (Figure 2A). To further support that CDYL is associated with both CAF-1 and MCM in cells,

Figure 1 The CAF-1 complex is physically associated with CDYL. (**A**) MS analysis of CDYL-associated proteins. U2OS cells stably expressing FLAG-CDYL were synchronized by a double thymidine block and released for 2 h. Cellular extracts were subsequently collected and subjected to affinity purification with anti-FLAG immobilized on the agarose beads. The eluates were resolved by SDS-PAGE and visualized by silver-staining. The bands were retrieved and analyzed by MS. (**B**) Western blotting of G9a, CDYL, MCM5, p60, and p150 in FLAG-CDYL-associated protein complex. (**C**) CDYL interacts with the CAF-1 complex *in vivo*. Whole-cell lysates from U2OS or HEK-293T cells were prepared, and IP was performed with anti-CDYL followed by IB with antibodies against p150, p60, and HA. (**D**) CDYL interacts directly with p150 *in vitro*. GST pull-down assays were performed with the indicated GST-CDYL fusion proteins and *in vitro* transcribed/translated p150, p60, and p48. (**E**) Mapping the molecular interface involved in the interaction between CDYL and p150. GST pull-down experiments were performed with a series of deletion mutants of CDYL and p150 as indicated. (**F**) Cell cycle-dependent colocalization of CDYL and p150. U2OS cells were transfected with GFP-p150 and FLAG-CDYL, synchronized by a double thymidine block, and released for indicated hours. Cells were fixed and immunostained with anti-FLAG antibody. Scale bar, 10 μm.

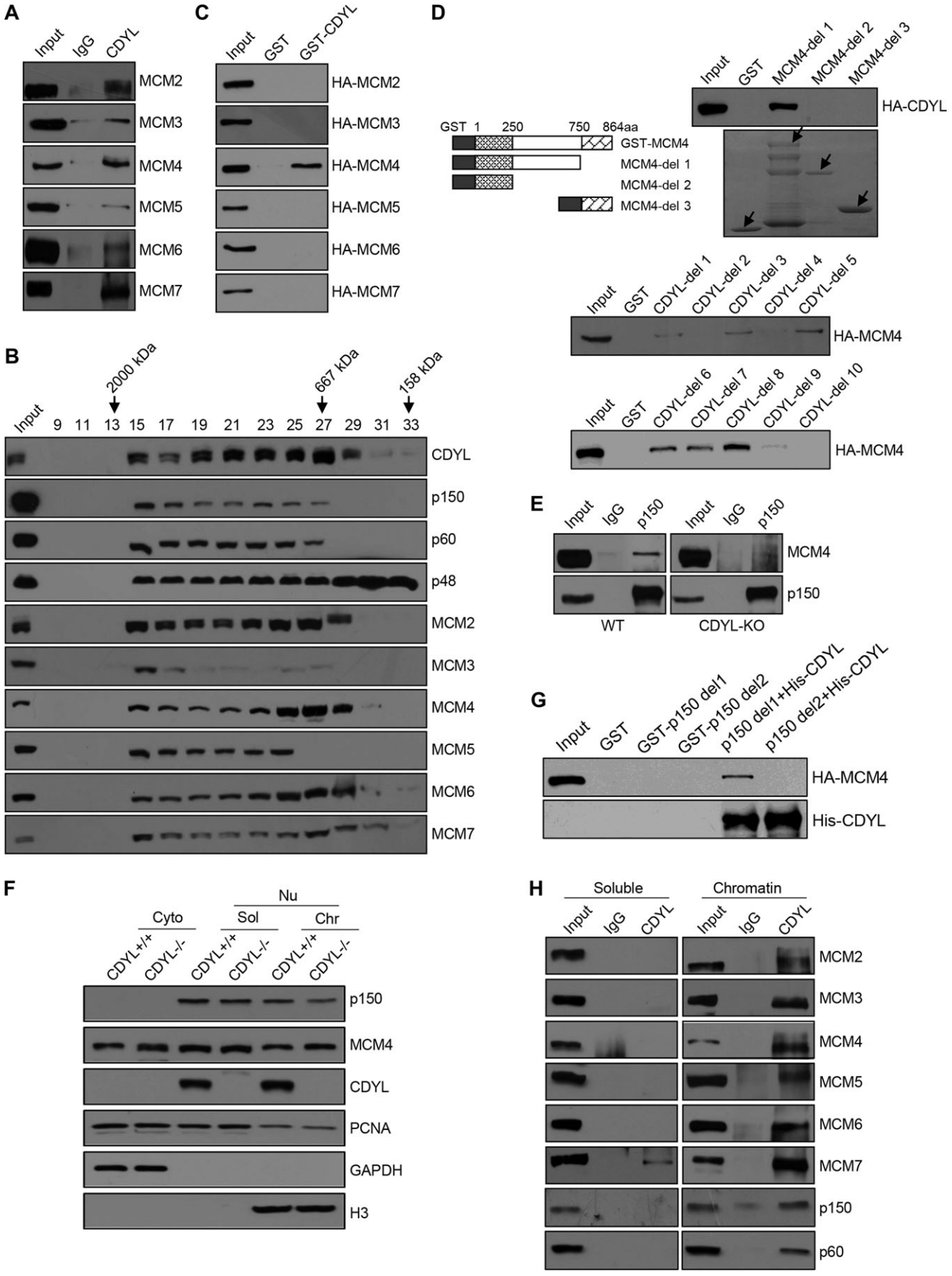

protein fractionation experiments were carried out by FPLC with Superose 6 columns and a high-salt extraction and size exclusion approach. Notably, native CDYL from U2OS cells was eluted with an apparent molecular mass much greater than that of the monomeric protein; CDYL immunoreactivity was detected in chromatographic fractions with a relatively symmetrical peak centered between ~667 and ~2000 kDa, an elution pattern largely overlapped with that of the components of CAF-1 and MCM complexes (Figure 2B), supporting that CDYL is associated with both complexes *in vivo*. Analogously, GST pull-down experiments showed that CDYL interacts directly with only MCM4, but not other MCM2–7 components (Figure 2C). Using a series of deletion mutants of CDYL and MCM4, we demonstrated that the region of 211–309 aa in CDYL and the region of 251–750 aa in MCM4 are responsible for their interaction (Figure 2D). Meanwhile, GST pull-down experiments revealed that none of the MCM2–7 components interacts directly with CAF-1 subunits (Supplementary Figure S1).

The observation that CDYL interacted with both CAF-1 and MCM without direct interaction between CAF-1 and MCM points to a scenario that CDYL serves as a bridging factor for the two complexes. To test this hypothesis, we established a somatic CDYL knockout (CDYL-KO) U2OS cell line using transcription activator-like effector nucleases (TALEN) technology (Sanjana et al., 2012) and examined whether depletion of CDYL would impair the interaction between CAF-1 and MCM. Western blotting and qRT-PCR confirmed the successful elimination of CDYL expression in CDYL-KO cells (Supplementary Figure S2). Co-IP assays showed that p150 subunit of CAF-1 interacted with MCM4 component of MCM in wild-type (WT) U2OS cells but not in CDYL-KO cells (Figure 2E), while neither the expression nor subcellular distribution of p150 and MCM4 protein was altered (Figure 2F). Moreover, *in vitro* reconstitution experiments conducted with purified recombinant proteins showed that MCM4 could be pulled down by GST-p150 only when His-CDYL was present in the reaction system (Figure 2G), further supporting that CDYL serves as a bridging factor for CAF-1 and MCM. Notably, IP assays performed with lysates of S-phase U2OS cells revealed that the interaction between CDYL and CAF-1 or MCM components could be detected predominantly in chromatin but not soluble fractions, indicating that CDYL interacts with both CAF-1 and MCM complexes mainly on chromatin (Figure 2H).

CDYL recruits KMTs G9a, SETDB1, and EZH2 to replication forks

Next, to test whether CDYL is recruited to replication sites, U2OS cells were transfected with GFP-CDYL construct, and intracellular localization of the fluorescent protein in S phase was examined. Cells were pre-extracted and fixed, and PCNA staining was performed to indicate replication sites, which were additionally labeled by 5-bromo-2-deoxyuridine (BrdU) staining. Confocal microscopy clearly showed that wild-type CDYL was almost completely co-localized with PCNA (Figure 3A). Notably, loss of either N-terminal chromodomain, which recognizes H3K9me2/3 and H3K27me2/3, or the middle region of CDYL, which interacts with replisome components p150 and MCM4, led to partial detachment of the protein from replication spots (Figure 3B), suggesting that both regions are required for anchoring CDYL to replication sites.

CDYL was previously reported to interact with EZH2 and G9a, two KMTs responsible for H3K27me3 and H3K9me1/2, respectively (Mulligan et al., 2008; Zhang et al., 2011). The formation of CAF-1–CDYL–MCM complex during S phase prompted us to examine whether this complex acts to recruit the KMTs to replication forks and plays a role in the transmission of the corresponding histone modifications in replicating chromatin. The physical association between CDYL and KMTs was first confirmed by co-IP assays performed with U2OS and HEK-293T cell lysates. We found that CDYL clearly interacts with G9a and EZH2 as expected, and also with SETDB1, which adds H3K9me3 mainly in euchromatin, whereas no interaction was detected between CDYL and SUV39H1, the KMT responsible for H3K9me3 in heterochromatin (Figure 3C). The direct interaction between CDYL and EZH2, G9a, or SETDB1 was further demonstrated by the GST pull-down assays (Figure 3D). Significantly, endogenous

Figure 2 CDYL links CAF-1 with MCM on chromatin. (**A**) Association of CDYL with the MCM complex in U2OS cells. Whole-cell lysates were subjected to IP with anti-CDYL followed by IB using antibodies against the indicated proteins. (**B**) Co-fractionation of CAF-1, CDYL, and MCM by FPLC. Cellular extracts from U2OS cells were fractionated on Superose 6 size exclusion columns. Chromatographic elution profiles and IB analysis of the chromatographic fractions are shown. The elution positions of calibration proteins with known molecular masses (kDa) are indicated, and equal volume from each fraction was analyzed. (**C**) CDYL directly interacts with MCM4 *in vitro*. GST pull-down assays were performed with the indicated GST-fused CDYL and *in vitro* transcribed/translated individual components of the MCM complex. (**D**) Mapping the molecular interface involved in the interaction between CDYL and MCM4 by GST pull-down experiments, with a series of deletion mutants of CDYL and MCM4 as indicated. (**E**) CDYL is required for the interaction between p150 and MCM4. Co-IP assays for p150 and MCM4 were performed in WT or CDYL-KO U2OS cells. (**F**) The distribution of CAF-1–CDYL–MCM components in different cell fractions. Cellular fractionation was performed in WT (CDYL+/+) or CDYL-KO (CDYL–/–) U2OS cells to separate cytoplasmic, nuclear-soluble, and chromatin fractions. Protein lysates from each fraction were subjected to IB with the indicated antibodies. GAPDH and H3 were used as loading controls. (**G**) CDYL mediates the interaction between p150 and MCM4 *in vitro*. Reconstitution GST pull-down assays were performed with indicated GST-p150 deletion mutants and *in vitro* transcribed/translated HA-MCM4, in the absence or presence of bacterially purified His-CDYL. (**H**) CDYL interacts with MCM and CAF-1 on chromatin. U2OS cells were synchronized by a double thymidine block and released for 3 h to allow cells to enter S phase. Soluble and chromatin-bound fractions were collected, and IP was performed with anti-CDYL followed by IB using antibodies against the indicated proteins.

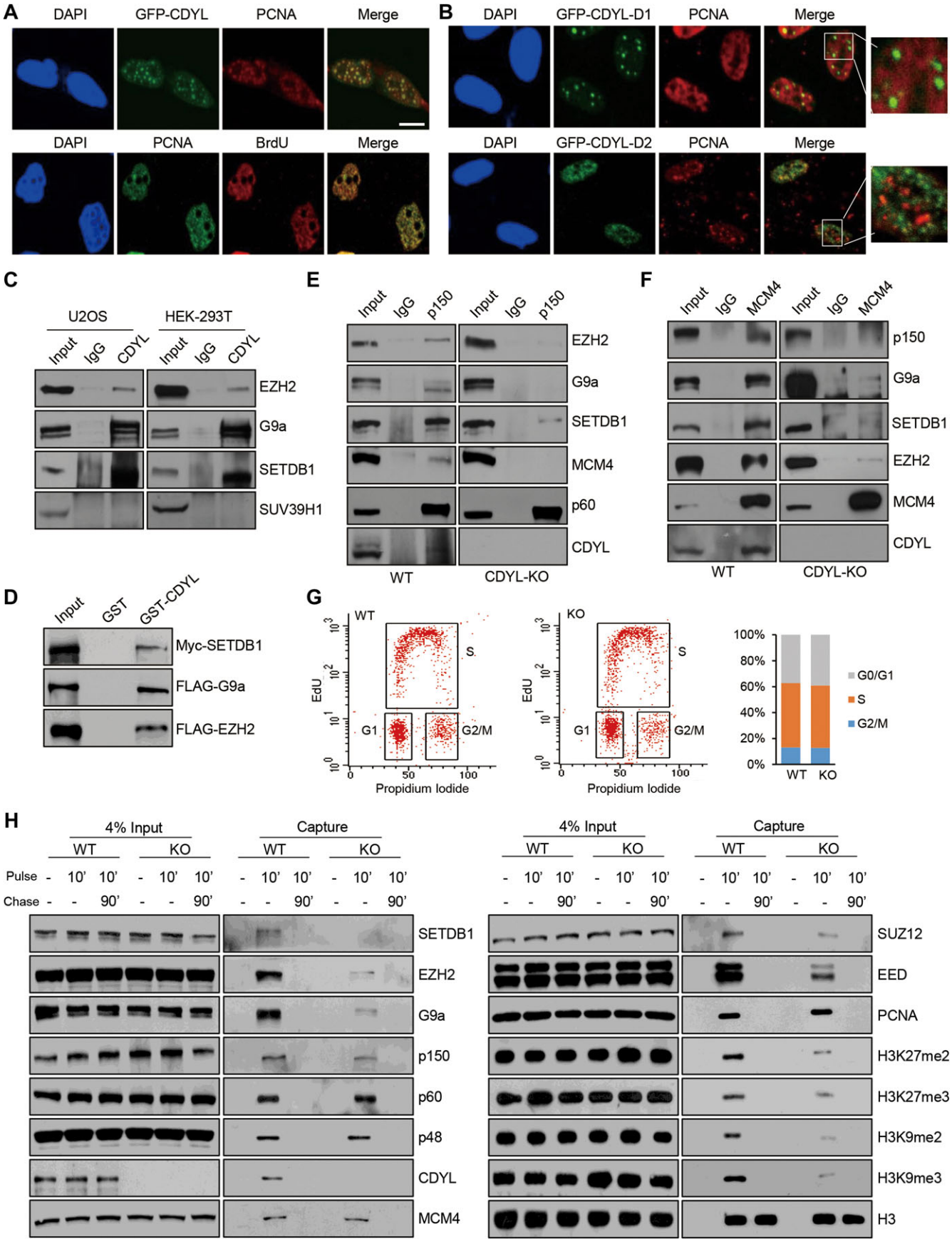

co-IP assays detected the physical association of p150 (CAF-1) with EZH2 and G9a in WT U2OS cells but not in CDYL-KO cells (Figure 3E). Likewise, physical interaction between MCM4 and EZH2 or G9a was detected in WT U2OS cells but not in CDYL-KO cells (Figure 3F). Collectively, these results support not only a role of CDYL in connecting CAF-1 and MCM complexes, but also a function of CDYL in the recruitment of KMTs by the CAF-1–CDYL–MCM machinery.

To further consolidate the association of CDYL with replication forks and examine its function in the recruitment of KMTs, we next utilized accelerated native isolation of proteins on nascent DNA (aniPOND) method (Sirbu et al., 2012; Leung et al., 2013; Aranda et al., 2014) to purify endogenous replication fork-associated proteins. To this end, U2OS cells were first pulse-labeled with thymidine analog 5-ethynyl-2-deoxyuridine (EdU) for 10 min, and the cells were subsequently chased for 90 min to detect proteins specifically associated with nascent DNA. The EdU incorporation in WT and CDYL-KO cells was monitored by FACS to ensure the equivalent capturing of EdU-labeled chromatin in the aniPOND assays (Figure 3G). As expected, histone H3, classic replication fork-associated protein PCNA, p150, p60, p48, and MCM4 were all detected by this method. Significantly, CDYL, G9a, SETDB1, as well as PRC2 components EZH2, SUZ12, and EED, were also readily detected in WT U2OS cells, supporting the coexistence of CDYL and these KMTs at replication forks (Figure 3H). Importantly, while CAF-1 components, MCM4, and PCNA were still detected by aniPOND analysis in CDYL-KO cells, the PRC2 components, G9a, and SETDB1 were largely diminished, accompanying with the significantly decreased replication fork-associated H3K9me2/3 and H3K27me2/3 in these cells (Figure 3H). Together, these data indicate that CDYL functions to recruit KMTs G9a, SETDB1, and PRC2 to replication forks and could play a role in the restoration/re-establishment of methylation of H3K9 and H3K27 during replication.

Restoration of H3K9me2/3 and H3K27me2/3 on newly assembled chromatin during S phase requires CDYL

We next analyzed the expression levels of CAF-1–CDYL–MCM components, CDYL-associated KMTs and histone modifications throughout the cell cycle. Western blotting revealed that the level of H3K27me3 gradually decreased from early to late S phase, consistent with a previous report (Lanzuolo et al., 2011). Interestingly, p150, CDYL, MCM4, and EZH2 displayed a similar pattern to that of H3K27me3, and the levels of H3K9me2/3 and G9a/SETDB1 followed a similar trend (Supplementary Figure S3), implying a functional connection between CAF-1–CDYL–MCM and the restoration/re-establishment of methylation of H3K9 and H3K27 during replication.

To further support this, we utilized the stable isotope labeling-based quantitative MS (SILAC) method (Chen et al., 2011; Xu et al., 2012) to examine whether depletion of CDYL would affect the establishment of H3K9me2/3 and H3K27me2/3 on newly deposited H3 (Figure 4A). Compared to WT U2OS cells, while the levels of unmodified histone peptides in CDYL-KO cells were not changed (Figure 4B), a significant delay in the establishment of H3K27me3 on new histones was observed upon CDYL depletion (Figure 4C). For example, at 6 h after G_1/S release, the ratio of Lys-6/Lys-0 (newly deposited histones/old histones) of H3K27me3 in WT cells was 0.135, whereas this ratio in CDYL-KO cells was only 0.039, ~28.9% of the normal value. Similar delay was also found for H3K27me2 and H3K9me2/3 establishment on new histones (Figure 4C). Since newly synthesized histones generally lack H3K27me2/3 and H3K9me2/3 pre-deposition (Almouzni and Cedar, 2016), the above data indicate that CDYL is required for the restoration of these repressive histone marks on daughter chromatin during replication. We also performed SILAC experiments in U2OS cells treated with specific siRNAs against p150 or MCM4. Compared to WT cells, depletion of MCM4 also caused significant delay in restoration of H3K27me2/3 and H3H9me2/3 on

Figure 3 CDYL recruits EZH2, G9a, and SETDB1 to replication forks. (**A**) CDYL is localized at sites of DNA replication. U2OS cells were transfected with GFP-CDYL, synchronized by a double thymidine block, and released for 3 h to allow cells to enter S phase. Cells were subsequently pulse-labeled with 20 μM BrdU for 15 min, pre-extracted, fixed, and stained. Denaturation step was applied for BrdU staining. Scale bar, 10 μm. (**B**) Both chromodomain and the middle region of CDYL are required for its localization at replication sites. U2OS cells were transfected with GFP-CDYL-D1 (mutant lack of N-terminal chromodomain) or GFP-CDYL-D2 (mutant lack of the middle 61–309 aa) and synchronized by a double-thymidine block. Cells were released for 3 h to enter S phase before pre-extracted, fixed, and stained with PCNA antibody. Scale bar, 10 μm. (**C**) CDYL interacts with EZH2, G9a, and SETDB1 *in vivo*. Whole-cell lysates from U2OS cells or HEK-293T cells were collected, and IP was performed with anti-CDYL followed by IB using antibodies against the indicated proteins. (**D**) CDYL directly interacts with EZH2, G9a, and SETDB1 *in vitro*. GST pull-down assays were performed with GST-fused CDYL and *in vitro* transcribed/translated FLAG-EZH2, FLAG-G9a, and Myc-SETDB1. (**E**) CDYL is required for the interaction between p150 and EZH2, G9a, and SETDB1. Co-IP assays for p150 and EZH2, G9a, SETDB1, MCM4, p60, and CDYL were performed in WT or CDYL-KO U2OS cells. (**F**) CDYL is required for the interaction between MCM4 and EZH2, G9a, and SETDB1. Co-IP assays for MCM4, and p150, G9a, SETDB1, EZH2, MCM4 and CDYL were performed in WT or CDYL-KO U2OS cells. (**G**) EdU incorporation assays were performed in WT and CDYL-KO (KO) cells. U2OS cells were incubated for 10 min with 10 μM EdU before the EdU incorporation was analyzed by flow cytometry. (**H**) CDYL is required to recruit PRC2 components (EZH2, SUZ12, and EED), G9a, and SETDB1 to replication forks. AniPOND experiments were performed in WT or CDYL-KO (KO) U2OS cells. Cells were pulsed with 10 μM EdU for 10 min. When indicated, pulsed cells were chased with 10 μM thymidine for 90 min after washing out the EdU. Cells were not treated with EdU in the control groups but a Click-IT reaction was performed. While CAF-1 components, PRC2 components, G9a, SETDB1, MCM4, and CDYL coexist at replication forks in WT cells, PRC2 components, G9a, and SETDB1 were largely diminished in KO cells. Meanwhile, the presence of H3K27me2/3 and H3K9me2/3 were also largely decreased at replication forks in KO cells. PCNA and H3 were used as positive controls.

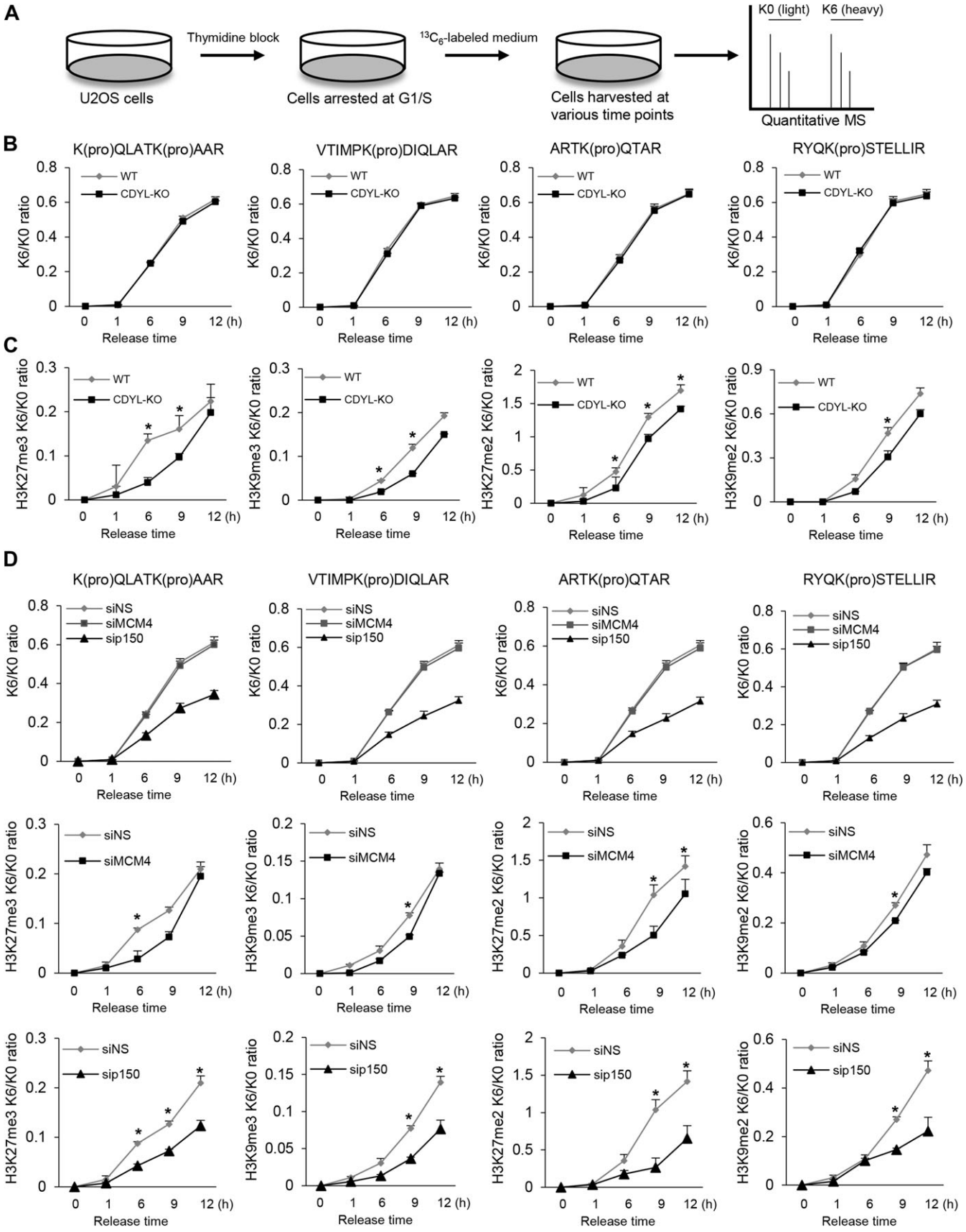

new chromatin without affecting the overall histone incorporation rate (Figure 4D). Notably, however, knockdown of p150 resulted in significantly reduced amount of newly synthesized H3 peptide, although a substantial delay of H3K27me2/3 and H3K9me2/3 establishment was also detected (Figure 4D). As CAF-1 is the major histone chaperone responsible for H3-H4 deposition, these observations probably reflect a feedback inhibition of histone synthesis due to the blockage of new histone incorporation. Together, the above data indicate that CDYL, as well as CAF-1 and MCM, are required for the restoration of H3K9me2/3 and H3K27me2/3 on newly assembled chromatin during S phase.

Depletion of CDYL and CAF-1 impairs the helicase activity of MCM

Transmission of H3K9me2/3 and H3K27me2/3 on newly assembled chromatin relies on efficient deposition of the 'seed', parental histones already labeled with these modifications (Campos et al., 2014). It has been reported that MCM helicase can act as the transient docking site of the released old histones (Groth et al., 2007a). Since we found that CDYL bridges the interaction between CAF-1 and MCM on replicating chromatin, it is possible that CAF-1–CDYL–MCM components coordinately transport and re-deposit parental $(H3\text{-}H4)_2$ tetramers, especially those with pre-existing H3K9me2/3 and H3K27me2/3 marks. We reasoned that if this is the case, disruption of CAF-1–CDYL–MCM machinery, by depletion of either CDYL or p150, could compromise the helicase activity of MCM, since timely removal of parental histones is required for continuous unwinding DNA in the context of chromatin. To test this hypothesis, U2OS cells were treated with hydroxyurea (HU), which depletes nucleotide pool and thus leads to the inhibition of DNA polymerase and formation of single-stranded DNA (ssDNA). Upon HU treatment, the majority of WT U2OS cells in S phase generated ssDNA patches, which were largely impeded in CDYL-KO cells and successfully restored by re-introduction of CDYL expression (Figure 5A), suggesting that the role of CDYL in this process is specific. Similarly, knockdown of p150 also led to impaired HU-induced ssDNA formation (Figure 5A). We additionally monitored ssDNA formation with replication protein A (RPA, which binds to ssDNA) binding assay (Groth et al., 2007a). Treating cells with HU resulted in a significant increase in acute RPA accumulation in pre-extracted S phase cells, whereas depletion of CDYL or pl50 led to a reduced response (Figure 5B). Loss of either CDYL or p150 did not affect RPA expression (Figure 5B, Supplementary Figure S4A), indicating that lack of RPA binding was due to lack of ssDNA formation.

We performed a series of experiments to rule out the possibility that lack of ssDNA formation in CDYL/p150-depleted cells is caused by indirect effects, such as reduced MCM complex recruitment, DNA damage at the replication fork, generally reduced fork progression, or reduced origin firing (Mejlvang et al., 2014). We first examined whether the amount of HU treatment would enhance DNA damage response in CDYL-KO cells. No evident γH2AX induction was found upon CDYL depletion, and HU treatment elicited similar increase in γH2AX levels in both WT and CDYL-KO cells (Supplementary Figure S4B). Depletion of CDYL neither affected the overall stability of the MCM complex on chromatin (Supplementary Figure S4C), nor disturbed the interaction between MCM and ASF1 (Supplementary Figure S4D), a chaperone that was previously reported to be involved in parental histone eviction (Groth et al., 2007a). Moreover, DNA fiber assays revealed that depletion of CDYL in U2OS cells had little effect on replication fork speed, whereas depletion of either p150 or MCM4 significantly hindered fork progression (Figure 5C). Depletion of CDYL also did not affect origin firing or other chromatin structures such as stalled fork or termination (Supplementary Figure S4E). These results suggest that the decrease in HU-induced ssDNA formation upon CDYL depletion is likely caused by hampered MCM helicase activity. Depletion of p150 or MCM4 delayed replication fork progression more significantly, which probably reflects their more general roles as replisome components.

Depletion of CDYL impedes early S phase progression and sensitizes cells to DNA damage

It was reported that knockdown of p150 leads to a reduced level of p60 component of CAF-1, suggesting that the stability of the CAF-1 complex is cooperatively regulated (Hoek and Stillman, 2003). Intriguingly, depletion of p150 in U2OS or HeLa cells also resulted in a decrease in CDYL levels, while the levels of MCM4, G9a, SETDB1, and EZH2 were not affected (Supplementary Figure S5A). qRT-PCR indicated that CDYL mRNA did not change, suggesting that the

Figure 4 CDYL is required for the establishment of H3K9me2/3 and H3K27me2/3 on newly deposited histone H3 during S phase. (**A**) Illustration of the SILAC-based quantitative MS method. In brief, U2OS cells were arrested with a double thymidine block. Cells were subsequently released for different hours in $[^{13}C_6]$ heavy isotope-labeled L-lysine (Lys-6)-supplemented medium to label newly synthesized proteins. Histone samples were acid-extracted (to release chromatin histones), resolved in 12% SDS-PAGE gel, and subjected to MS analysis. (**B**) Total incorporation of newly synthesized histones is not changed in CDYL-KO cells. The K6/K0 ratio (represents new/old) of representative H3.1 backbone peptides was calculated according to MS data in WT and CDYL-KO cells. Pro, propionylation. (**C**) Depletion of CDYL impairs establishment of H3K27me2/3 and H3K9me2/3 on newly deposited histones. The K6/K0 ratio of histone peptides modified with H3K27me2/3 and H3K9me2/3 was calculated according to MS data in WT and CDYL-KO cells. (**D**) Depletion of p150 or MCM4 impairs establishment of H3K27me2/3 and H3K9me2/3 on newly deposited histones. U2OS cells were transfected with specific siRNAs against p150 or MCM4. The K6/K0 ratio of H3.1 backbone peptides or histone peptides modified with H3K27me2/3 and H3K9me2/3 was calculated according to MS data. Note upon p150 depletion, total incorporation of newly synthesized histones was also significantly impaired. Error bars represent mean ± SD for triplicate experiments. $^*P < 0.05$.

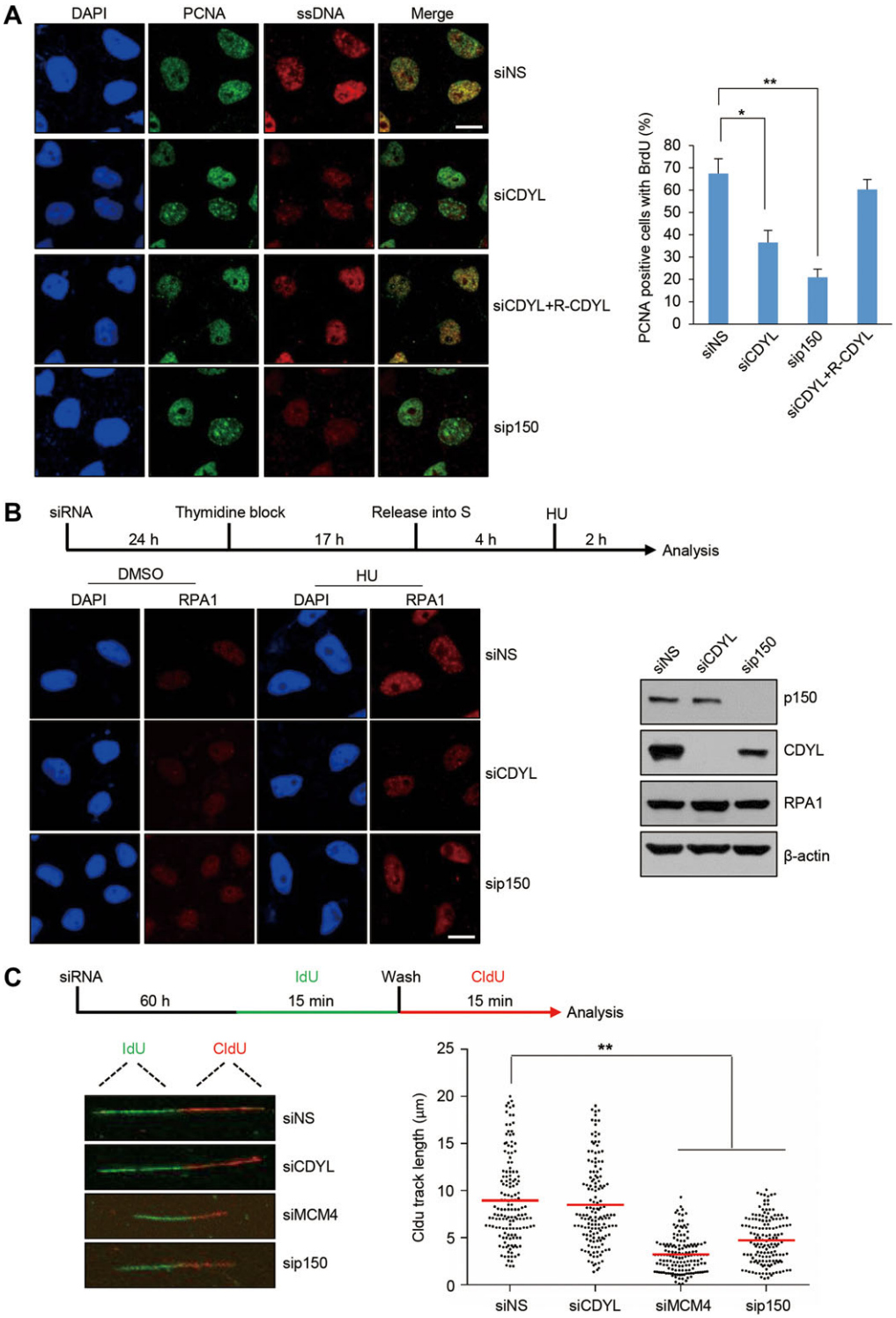

Figure 5 Depletion of CDYL or p150 impairs DNA unwinding. (**A**) ssDNA formation in siRNA-treated U2OS cells after HU treatment. BrdU (20 μg/ml) was added during the last 24 h of siRNA treatment and was removed by a brief wash prior to HU treatment (4 mM, 2 h), pre-extraction, and fixation. BrdU in ssDNA patches and PCNA were detected without a DNA denaturation step. Scale bar, 10 μm. Diagrams show the frequency of PCNA-positive BrdU foci. Bars represent mean ± SD for triplicate experiments. *$P < 0.05$, **$P < 0.01$, two-tailed unpaired *t*-test. (**B**) Depletion of CDYL or p150 reduces chromatin-bound RPA1 upon HU treatment. The experimental design is shown. Cells were transfected, synchronized, released into S phase for 4 h, and treated with HU for 2 h. RPA1 staining in pre-extracted cells was reduced upon CDYL/p150 depletion, while total PRA protein levels were not changed. Scale bar, 10 μm. (**C**) DNA fiber analysis of the rate of replication elongation. siRNA-treated U2OS cells were sequentially pulse-labeled with 50 μM IdU and 50 μM CldU, each for 15 min. A sketch delineating experimental design and representative images of dual-labeled fibers are shown. Green tracts, IdU; red tracts, CldU. CldU tract length was counted. Bars represent the median ($n = 300$ in each group). **$P < 0.01$, two-tailed unpaired *t*-test.

decrease of CDYL expression upon p150 knockdown occurs at the protein level (Supplementary Figure S5B). Treating p150-depleted cells with proteasome inhibitor MG132 stabilized CDYL protein, indicating that the decrease of CDYL is due to proteasomal degradation (Supplementary Figure S5C). Meanwhile, knockdown of CDYL did not affect p150 or MCM4, and knockdown of MCM4 did not affect p150 or CDYL (Supplementary Figure S5D). These data support a close functional connection between CDYL and CAF-1, suggesting that p150 might represent the central regulatory node for the overall stability of the CAF-1–CDYL–MCM complex.

To extend our observations to a physiologically relevant response, we determined the effect of depletion of CDYL, as well as CAF-1 and MCM, on the growth and proliferation of U2OS cells. FACS analysis revealed similar cell cycle profile of unsynchronized CDYL-KO cells compared to WT U2OS cells (Supplementary Figure S6A). BrdU incorporation and FACS examination of synchronized cells indicated that depletion of CDYL resulted in a significant delay in early S phase but not the overall S phase progression, and re-expression of CDYL in CDYL-KO cells successfully rescued this effect (Figure 6A–C). Consistent with previous reports (Hoek and Stillman, 2003; Ibarra et al., 2008) and the general role of CAF-1 and MCM in replication, depletion of either p150 or MCM4 by specific siRNAs also significantly impaired early to middle S phase progression (Supplementary Figure S6B–D).

Since re-establishment of epigenetic modifications during replication is also vital for the maintenance of genome stability (Yang et al., 2011), we next analyzed the effect of depletion of CDYL, as well as CAF-1 or MCM, on the survival of U2OS cells responding to genetic insult. To this end, p150-, MCM4-, or CDYL-deficient U2OS cells were treated with camptothecin (CPT), which abolishes the religation activity of topoisomerase I and thus leads to double-strand break, replication fork collision, and S phase arrest (Regairaz et al., 2011), or cytotoxic anticancer drug etoposide (VP16), which damages DNA by inhibition of the religation activity of topoisomerase II (Adachi et al., 2003). Flow cytometry showed that U2OS cells deficient of p150, CDYL, or MCM4 exhibited a significant higher rate of apoptosis when exposed to CPT, but showed less change on VP16-induced apoptosis (Figure 6D). Consistent with the above data, western blotting revealed that treatment with CPT, but not VP16, increased levels of γH2AX induction in CDYL-, p150-, or MCM4-depleted cells (Figure 7A).

CPT activates S or G_2-M arrest and homologous recombination (HR) repair in tumor cells, whereas VP16 damages DNA without affecting a particular cell cycle phase, and thus elicits mainly nonhomologous end joining (NHEJ) repair pathway (Adachi et al., 2003; Yang et al., 2013). The differential cell response to CPT versus VP16 upon CDYL depletion led us to conceive that the CAF-1–CDYL–MCM machinery could be involved in HR rather than NHEJ repair pathway. To test this, we used GFP-based chromosomal reporter assays with two stable cell lines, DR-GFP-U2OS and EJ5-GFP-HEK293, both of which have been well-established to measure HR or NHEJ, respectively (Yang et al., 2013; Li et al., 2014). Knockdown of CDYL was associated with a significant decrease in the percentage of GFP^+ DR-U2OS cells, an effect that could be rescued by overexpression of a siRNA-resistant CDYL construct (Figure 7B). Likewise, knockdown of p150 or MCM4 also resulted in a significant reduction in the percentage of GFP^+ DR-U2OS cells (Figure 7B). By contrast, no significant changes were observed for the efficiency of total NHEJ in CDYL-deficient EJ5-HEK293 cells (Figure 7C), suggesting that CDYL, together with CAF-1 and MCM, is involved in HR but not NHEJ repair pathway. Furthermore, ChIP analysis clearly showed that CDYL, MCM4, and p150 were indeed all enriched at DNA damage sites in DR-GFP-U2OS cells (Figure 7D). Knockdown of p150 led to diminished local enrichment of CDYL, suggesting that CDYL is targeted to DNA damage sites through its interaction with p150 (Figure 7E). Significantly, knockdown of CDYL abolished the recruitment of EZH2, G9a, and SETDB1 and the concomitant local enrichment of H3K9me2/3 and H3K27me2/3 (Figure 7F), suggesting that CDYL is functional at these sites. Together, the above data support the argument that CDYL plays an important role in the maintenance of genome stability.

Discussion

Maintenance and inheritance of epigenetic information with a high fidelity is a great challenge to all proliferating cells. Despite its importance, the underlying molecular mechanism of epigenetic inheritance, in particular the maintenance of dynamic histone modifications is less clear. It is thought that transcriptionally active histone modifications on parental nucleosomes are not necessarily duplicated in a replication-coupled manner, as long as a permissive chromatin structure is sufficiently maintained, such that new nucleosomes will acquire active marks when transcription resumes (Groth et al., 2007b). By contrast, epigenetic domains enriched with repressive histone modifications, such as methylation of H3K9 and H3K27, are more critical to be faithfully inherited as they are essential for proper chromosome segregation and maintenance of cell identity (Zhu and Reinberg, 2011; Alabert and Groth, 2012). A classic example of histone modification inheritance is HP1-mediated H3K9me3 propagation in heterochromatin (Hathaway et al., 2012). Previous studies also suggest that pre-existing DNA methylation could contribute to replication-coupled restoration of H3K9 methylation mediated by KMTs SETDB1 and G9a (Sarraf and Stancheva, 2004; Esteve et al., 2006). Specifically, SETDB1 could be recruited by methyl-CpG binding protein MBD1 to p150, facilitating stable heterochromatin formation during replication (Sarraf and Stancheva, 2004); whereas G9a and DNMT1 are loaded onto replication foci by PCNA to coordinate DNA and histone methylation (Esteve et al., 2006). Whether a self-propagation mechanism exists for SETDB1/G9a-mediated H3K9 methylation is not clear. In the case of H3K27me3, researchers have proposed that EED subunit of PRC2 is responsible for the propagation of this modification on chromatin (Hansen et al., 2008; Margueron et al., 2009). However, the relatively low binding affinity of EED for H3K27me3 (Vermeulen et al., 2010; Xu et al., 2010) and lack of evidence that EED can bind to any replisome components in mammalian cells (Margueron et al., 2009) leave open whether EED is the major molecule in charge of H3K27me3 inheritance.

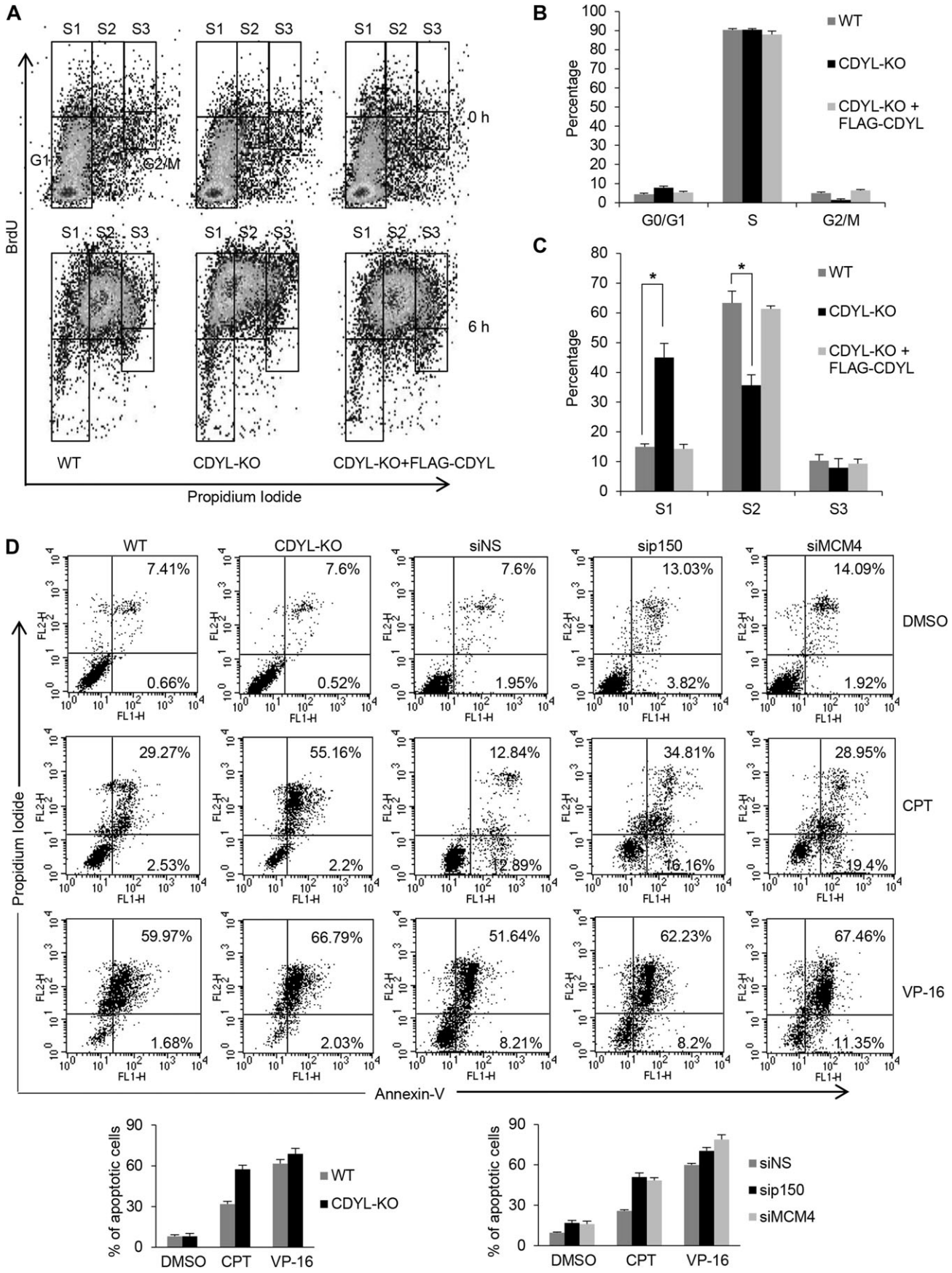

In this report, we identified chromodomain protein and transcription corepressor CDYL, through its interaction with histone chaperone CAF-1 and DNA helicase MCM during replication, as a key player in mediating the inheritance and maintenance of H3K9me2/3 and H3K27me2/3. The role of CDYL in many ways mimics the action of HP1, as both proteins contain chromodomain that recognizes repressive histone methylation; both proteins directly interact with KMTs (CDYL interacts with G9a, SETDB1, and EZH2, whereas HP1 interacts with SUV39H1); and both proteins directly interact with p150 subunit of CAF-1 during replication, but no direct interaction was found between EED and p150 (Supplementary Figure S7). The strong enrichment of CDYL in replicating chromatin is also supported by a recent study using nascent chromatin capture (NCC) to profile chromatin proteome dynamics during S phase (Alabert et al., 2014). Compared to MBD1 and DNMT1, two factors previously reported to recruit SETDB1 and G9a to replication sites (Sarraf and Stancheva, 2004; Esteve et al., 2006), CAF-1–CDYL–MCM-mediated histone modification inheritance does not require pre-existing DNA methylation, suggesting that this machinery possibly functions in less compact chromatin regions. Consistently, depletion of CDYL mainly impedes progression of early S phase (Figure 6A–C), when replication of euchromatin rather than the more condensed heterochromatin takes place (Alabert and Groth, 2012).

It was previously thought CAF-1 is mainly responsible for the deposition of newly-synthesized H3-H4, which are associated with histone chaperone ASF1, onto replicating DNA for *de novo* chromatin assembly (Campos et al., 2014; Almouzni and Cedar, 2016). Whether CAF-1 is involved in parental H3-H4 transfer is not clear. Unlike new histones, which are transferred and deposited in dimers for both H2A-H2B and H3-H4, parental nucleosomes are generally disrupted into two H2A-H2B dimers and one $(H3\text{-}H4)_2$ tetramer, which are then re-assembled on daughter strands (Groth et al., 2007b; Alabert and Groth, 2012). Because H2A-H2B dimers are susceptible to internucleosomal exchange throughout interphase, the $(H3\text{-}H4)_2$ tetrameric core is the likely candidate for transmitting epigenetic information (Campos et al., 2014). How parental $(H3\text{-}H4)_2$ tetramers are transferred remains unclear. Evidence suggests that MCM helicase can serve as a transient docking site of released histones, and histone chaperone ASF1 interacts with MCM through a histone H3-H4 bridge and thus could handle parental histones at the replication fork (Groth et al., 2007a). However, the binding interface between ASF1 and the histone dimer hinders the formation of H3-H3' contacts seen within $(H3\text{-}H4)_2$ tetramer (English et al., 2006), countering in favor of a conservative segregation of nucleosomal histones. Other studies, mainly in yeast, propose that MCM interacts with FACT to facilitate direct transfer of parental histones (Abe et al., 2011; Foltman et al., 2013). However, FACT is predominantly viewed as a H2A-H2B chaperone, although some researchers suggest that it can bind to all four histones (Belotserkovskaya et al., 2003; Stuwe et al., 2008). Our current evidence suggests that the CAF-1–CDYL–MCM machinery at the replication fork could play a role in transfer of parental $(H3\text{-}H4)_2$ tetramers, which carry pre-existing H3K9me2/3 and H3K27me2/3, because the functional specificity of this machinery likely comes from CDYL. Further reconstitution assays are needed to solidify this proposal.

The role of CDYL in mediating the transmission of H3K9me2/3 and H3K27me2/3 is not likely due to its influence on the early S phase progression, as depletion of CDYL in cells does not affect the incorporation rate of H3K4me3, another histone modification existed in euchromatin and mainly established during early S phase (Supplementary Figure S8A). Further dissecting the molecular details of CDYL in mediating its interactions with KMTs, p150, or MCM4 and generating specific CDYL point mutations should help to clarify the pleiotropic role of CDYL during replication, although the overlapping CDYL domains responsible for its interactions with respective proteins make systematic mutagenesis analysis somewhat difficult (Figures 1E, 2D, and Supplementary Figure S8B). Additionally, it is noted that CDYL can form multimers (Supplementary Figure S8C–E), a feature similar to HP1 that might play a role in bridging nucleosomes to couple parental histone release and *de novo* chromatin assembly for faithful restoration of epigenetic information (Brasher et al., 2000). Under this circumstance, whether CAF-1 also plays a role in duplicating H3K9me2/3 and H3K27me2/3 on new histones is less clear. However, we showed that depletion of p150 resulted in degradation of both p60 (Hoek and Stillman, 2003) and CDYL, indicating that the functional connection between CDYL and CAF-1 is tight. Therefore, we propose CAF-1 and CDYL may work together to propagate repressive histone modifications along newly assembled chromatin (Supplementary Figure S9).

Transmission of epigenetic memories across generations faces daunting challenges, as gross chromatin remodeling events constantly occur during DNA replication, mitosis, meiosis, and developmental reprogramming. While our study suggests that dedicated mechanism exists to restore H3K27me2/3 and H3K9me2/3 in a replication-coupled manner, these data do not exclude that re-establishment of these marks could be a

Figure 6 Depletion of CDYL inhibits cell cycle progression and sensitizes cells to DNA damage. (**A**) Depletion of CDYL inhibits cell cycle progression through early S phase. WT or CDYL-KO U2OS cells were synchronized by a double thymidine block and released for 6 h. Cells were labeled with 30 μM BrdU for 20 min and stained with BrdU antibody and propidium iodide (PI) for flow cytometry analysis. S phase was divided into three sub-S phases (early-S1, mid-S2, and late-S3) as indicated. (**B** and **C**) Summary of the above results showing cell cycle distribution in different phases (G_0/G_1, S, and G_2/M) or sub-S phases (S1, S2, and S3), respectively. Bars represent mean ± SD for triplicate experiments. *$P < 0.05$, Student's *t*-test. (**D**) Depletion of CDYL, p150, or MCM4 promotes cell apoptosis. WT U2OS cells or cells depleted of CDYL, p150, or MCM4 were treated with 1 μM CPT or 40 nM VP16 for 36 h, and then double-stained with annexin V and propidium iodide. Cell apoptosis was determined by flow cytometry. Bars represent mean ± SD for three independent experiments.

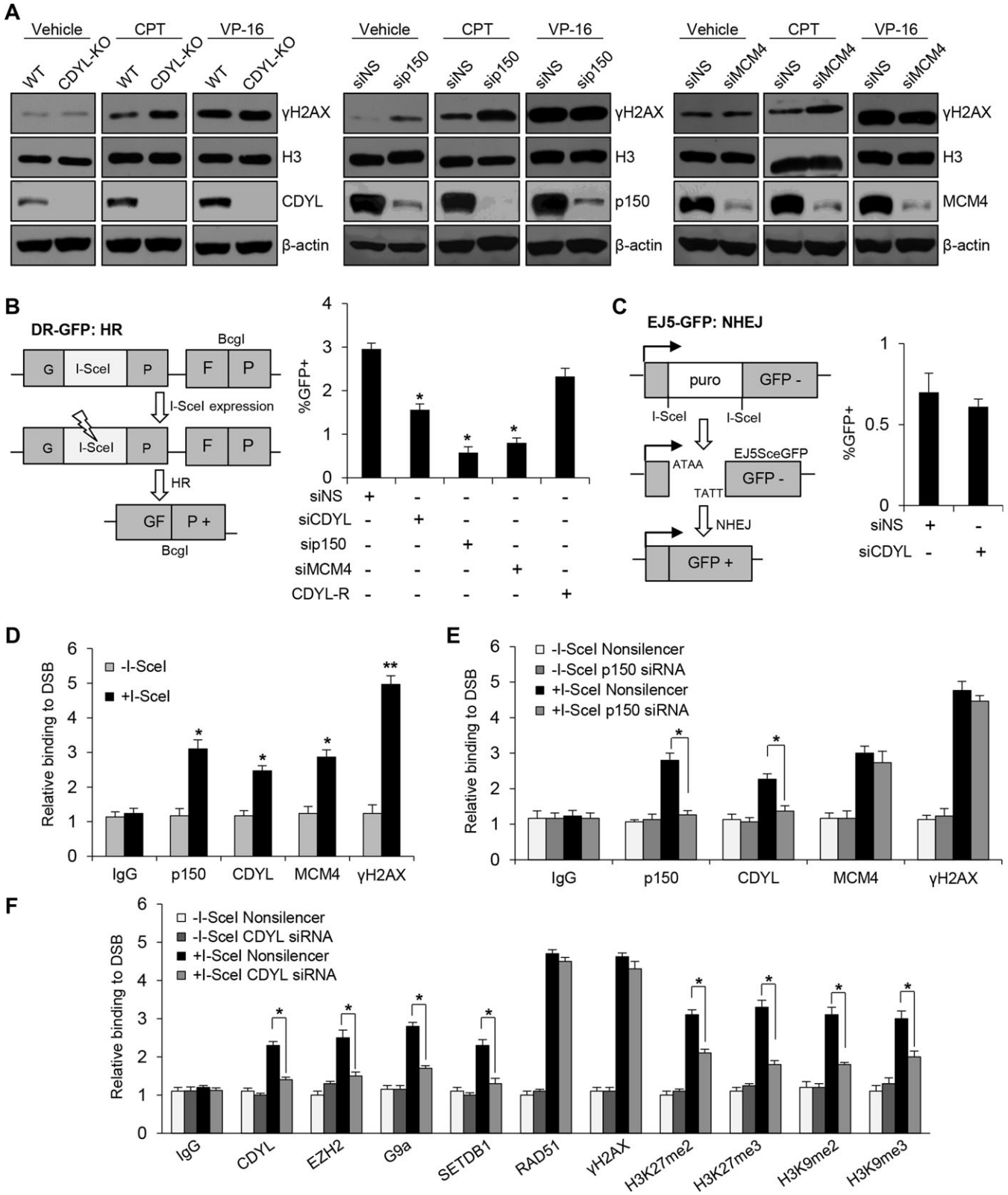

Figure 7 CDYL is important for genome stability. (**A**) Accumulation of γH2AX in cells depleted of CDYL, p150, or MCM4 after CPT stimulation. U2OS cells were treated with 1 μM CPT or 40 μM VP16 for 8 h before harvesting. Cell lysates were analyzed by IB. (**B**) CDYL is required for HR-mediated DNA repair. Schematic illustration of I-SceI-mediated double-strand break induction and repair using DR-GFP transgenes is shown. Cells were transfected with control, CDYL siRNA, p150 siRNA, MCM4 siRNA, or CDYL siRNA together with siRNA-resistant CDYL

continuous process extended throughout the cell cycle (Aoto et al., 2008; Xu et al., 2012; Alabert et al., 2014). The different cell cycle-dependent dynamics of the histone modifications observed by us (Supplementary Figure S3) versus others (Xu et al., 2012) could be due to different intervals and methods of sample collection. Beyond S phase, CDYL can still participate in the transmission of H3K27me3 and H3K9me3 along chromatin, as long as the protein reads these modifications and associates with the corresponding methyltransferases (Hathaway et al., 2012). In this sense, acquiring cellular memory through histone-binding proteins could be a two-wave process: initial segregation at the replication fork and post-replicative recruitment to their genomic targets as chromatin matures (Zee et al., 2012). Importantly, we demonstrated that CDYL also plays a role in HR repair (Figure 7). Thus, whether CDYL functions to promote transcription inhibition to avoid negatively interference between active transcription and the repair machineries, and/or helps to restore chromatin structure after repair, awaits further investigation (Soria et al., 2012). While homologs of CDYL have been previously implicated to play a role in spermatogenesis (Lahn et al., 2002) and be associated with certain types of cancers (www.oncomine.org), it will be interesting to use *in vivo* animal models to further investigate how the role of CDYL in transmitting repressive histone marks demonstrated in cultured cell lines could be implicated under these developmental or pathological conditions. Nevertheless, our study demonstrates that by interacting with CAF-1 and MCM, CDYL plays an important role in the maintenance of repressive histone marks during replication, providing a mechanism for understanding of the epigenetic inheritance and memory.

Materials and methods

TALEN-mediated CDYL knockout

A TALEN binding pair was chosen from CDYL gene in the second exon between GTT222964 and AAG223630 (total 667 bp), because the first exon of CDYL is too short (total 24 bp). The genomic recognition sequences of TALEN left and right arms are GAGGAATACATCCACGAC (L) and GCTCTCCTTCTGCTTCTC (R), spaced by 16 bp and anchored by a preceding T base at the −1 position to meet the optimal criteria for natural TAL proteins (Boch et al., 2009; Moscou and Bogdanove, 2009; Sanjana et al., 2012). TALEN vectors of left and right arms, TALEN-CDYL-L and TALEN-CDYL-R, were obtained by one-step ligation using FastTALE™ TALEN assembly kit (SIDANSAI Biotechnology) according to the manufacturer's instructions. U2OS and HeLa cells were transfected with the two TALEN-CDYL vectors. Puromycin-resistant cell clones were analyzed by PCR, and DNA sequencing was performed to confirm CDYL deletion.

SILAC-based quantitative MS

U2OS cells were arrested with a double thymidine block (2 mM thymidine for 17 h, released for 12 h, followed by a second treatment of 2 mM thymidine for 17 h). The cells were subsequently released into Lys-6 ([$^{13}C_6$] heavy isotope-labeled L-lysine)-supplemented medium for labeling. Total histones were isolated from cells using acid extraction (Shechter et al., 2007). In brief, cells were lysed with hypotonic lysis buffer (10 mM Tris-HCl, pH 8.0, 1 mM KCl, 1.5 mM $MgCl_2$, 1 mM DTT, and protease and phosphatase inhibitors added just before use) and subsequently incubated for 30 min on rotator at 4°C. After centrifugation, the supernatant was removed with pipette, and the pellet was resuspended in 0.4 N H_2SO_4. Histone samples were resolved using 12% SDS-PAGE gels and subjected to MS analysis. For stable isotope labeling-based quantification, the retrieved results from Mascot were analyzed by MSQuant to calculate the ratios for the heavy/light peptide pairs.

More methods can be found in Supplementary material.

Supplementary material

Supplementary material is available at *Journal of Molecular Cell Biology* online.

Funding

This work was supported by grants from the 973 Program of the Ministry of Science and Technology of China (2014CB542004 to J.L. and 2016YFC1302304 to Y.S.), and the National Natural Science Foundation of China (31371301 and 81572771 to J.L.; 91219201 and 81130048 to Y.S.).

Conflict of interest: none declared.

construct (CDYL-R), and FACS analysis of the relative repair rate in the treated DR-GFP U2OS cells is shown. Bars represent mean ± SD for triplicate experiments. * $P < 0.05$, Student's *t*-test. (**C**) CDYL is not required for NHEJ-mediated DNA repair. Schematic illustration of I-SceI-mediated double-strand break induction and repair using EJ5-GFP transgenes is shown. Cells were treated with control or CDYL siRNA, and FACS analysis of the relative repair rate is shown. Bars represent mean ± SD for triplicate experiments. (**D**) CDYL is present at DNA damage sites during HR. DR-GFP U2OS cells were induced for HR as in **B**, and ChIP analysis was performed with indicated antibodies. DNA damage sites were identified using specific primers described in Supplementary Material and Methods. The ChIP assays were analyzed for folds of enrichment relative to IgG. *$P < 0.05$, **$P < 0.01$, Student's *t*-test. (**E**) CDYL is targeted to DNA damage sites through p150. DR-GFP U2OS cells were induced for HR as in **B**. Cells were transfected with control or p150 siRNA, and ChIP analysis was performed as in **D**. Bars represent mean ± SD for triplicate experiments. *$P < 0.05$, Student's *t*-test. (**F**) Depletion of CDYL impairs the recruitment of repressive KMTs at DNA damage sites. DR-GFP U2OS cells were induced for HR, and transfected with control or CDYL siRNA. ChIP analysis was performed with indicated antibodies. Knockdown of CDYL did not affect the recruitment of early repair factor RAD51, whereas the recruitment of EZH2, G9a, and SETDB1 at DNA damage sites were decreased. Bars represent mean ± SD for triplicate experiments. *$P < 0.05$, Student's *t*-test.

References

Abe, T., Sugimura, K., Hosono, Y., et al. (2011). The histone chaperone facilitates chromatin transcription (FACT) protein maintains normal replication fork rates. J. Biol. Chem. *286*, 30504–30512.

Adachi, N., Suzuki, H., Iiizumi, S., et al. (2003). Hypersensitivity of nonhomologous DNA end-joining mutants to VP-16 and ICRF-193: implications for the repair of topoisomerase II-mediated DNA damage. J. Biol. Chem. *278*, 35897–35902.

Alabert, C., Bukowski-Wills, J.C., Lee, S.B., et al. (2014). Nascent chromatin capture proteomics determines chromatin dynamics during DNA replication and identifies unknown fork components. Nat. Cell Biol. *16*, 281–293.

Alabert, C., and Groth, A. (2012). Chromatin replication and epigenome maintenance. Nat. Rev. Mol. Cell Biol. *13*, 153–167.

Almouzni, G., and Cedar, H. (2016). Maintenance of epigenetic information. Cold Spring Harb. Perspect. Biol. *8*, pii: a019372.

Aoto, T., Saitoh, N., Sakamoto, Y., et al. (2008). Polycomb group protein-associated chromatin is reproduced in post-mitotic G1 phase and is required for S phase progression. J. Biol. Chem. *283*, 18905–18915.

Aranda, S., Rutishauser, D., and Ernfors, P. (2014). Identification of a large protein network involved in epigenetic transmission in replicating DNA of embryonic stem cells. Nucleic Acids Res. *42*, 6972–6986.

Bartke, T., Vermeulen, M., Xhemalce, B., et al. (2010). Nucleosome-interacting proteins regulated by DNA and histone methylation. Cell *143*, 470–484.

Belotserkovskaya, R., Oh, S., Bondarenko, V.A., et al. (2003). FACT facilitates transcription-dependent nucleosome alteration. Science *301*, 1090–1093.

Boch, J., Scholze, H., Schornack, S., et al. (2009). Breaking the code of DNA binding specificity of TAL-type III effectors. Science *326*, 1509–1512.

Bochman, M.L., and Schwacha, A. (2009). The Mcm complex: unwinding the mechanism of a replicative helicase. Microbiol. Mol. Biol. Rev. *73*, 652–683.

Bonasio, R., Tu, S., and Reinberg, D. (2010). Molecular signals of epigenetic states. Science *330*, 612–616.

Brasher, S.V., Smith, B.O., Fogh, R.H., et al. (2000). The structure of mouse HP1 suggests a unique mode of single peptide recognition by the shadow chromo domain dimer. EMBO J. *19*, 1587–1597.

Campos, E.I., Stafford, J.M., and Reinberg, D. (2014). Epigenetic inheritance: histone bookmarks across generations. Trends Cell Biol. *24*, 664–674.

Chen, X., Xiong, J., Xu, M., et al. (2011). Symmetrical modification within a nucleosome is not required globally for histone lysine methylation. EMBO Rep. *12*, 244–251.

English, C.M., Adkins, M.W., Carson, J.J., et al. (2006). Structural basis for the histone chaperone activity of Asf1. Cell *127*, 495–508.

Esteve, P.O., Chin, H.G., Smallwood, A., et al. (2006). Direct interaction between DNMT1 and G9a coordinates DNA and histone methylation during replication. Genes Dev. *20*, 3089–3103.

Foltman, M., Evrin, C., De Piccoli, G., et al. (2013). Eukaryotic replisome components cooperate to process histones during chromosome replication. Cell Rep. *3*, 892–904.

Franz, H., Mosch, K., Soeroes, S., et al. (2009). Multimerization and H3K9me3 binding are required for CDYL1b heterochromatin association. J. Biol. Chem. *284*, 35049–35059.

Groth, A., Corpet, A., Cook, A.J., et al. (2007a). Regulation of replication fork progression through histone supply and demand. Science *318*, 1928–1931.

Groth, A., Rocha, W., Verreault, A., et al. (2007b). Chromatin challenges during DNA replication and repair. Cell *128*, 721–733.

Hansen, K.H., Bracken, A.P., Pasini, D., et al. (2008). A model for transmission of the H3K27me3 epigenetic mark. Nat. Cell Biol. *10*, 1291–1300.

Hathaway, N.A., Bell, O., Hodges, C., et al. (2012). Dynamics and memory of heterochromatin in living cells. Cell *149*, 1447–1460.

Hoek, M., and Stillman, B. (2003). Chromatin assembly factor 1 is essential and couples chromatin assembly to DNA replication in vivo. Proc. Natl Acad. Sci. USA *100*, 12183–12188.

Ibarra, A., Schwob, E., and Mendez, J. (2008). Excess MCM proteins protect human cells from replicative stress by licensing backup origins of replication. Proc. Natl Acad. Sci. USA *105*, 8956–8961.

Kaufman, P.D., Kobayashi, R., Kessler, N., et al. (1995). The p150 and p60 subunits of chromatin assembly factor I: a molecular link between newly synthesized histones and DNA replication. Cell *81*, 1105–1114.

Lahn, B.T., Tang, Z.L., Zhou, J., et al. (2002). Previously uncharacterized histone acetyltransferases implicated in mammalian spermatogenesis. Proc. Natl Acad. Sci. USA *99*, 8707–8712.

Lanzuolo, C., Lo Sardo, F., Diamantini, A., et al. (2011). PcG complexes set the stage for epigenetic inheritance of gene silencing in early S phase before replication. PLoS Genet. *7*, e1002370.

Leung, K.H., Abou El Hassan, M., and Bremner, R. (2013). A rapid and efficient method to purify proteins at replication forks under native conditions. Biotechniques *55*, 204–206.

Li, X., Liu, L., Yang, S., et al. (2014). Histone demethylase KDM5B is a key regulator of genome stability. Proc. Natl Acad. Sci. USA *111*, 7096–7101.

Margueron, R., Justin, N., Ohno, K., et al. (2009). Role of the polycomb protein EED in the propagation of repressive histone marks. Nature *461*, 762–767.

Margueron, R., and Reinberg, D. (2011). The Polycomb complex PRC2 and its mark in life. Nature *469*, 343–349.

Mejlvang, J., Feng, Y., Alabert, C., et al. (2014). New histone supply regulates replication fork speed and PCNA unloading. J. Cell Biol. *204*, 29–43.

Moscou, M.J., and Bogdanove, A.J. (2009). A simple cipher governs DNA recognition by TAL effectors. Science *326*, 1501.

Mulligan, P., Westbrook, T.F., Ottinger, M., et al. (2008). CDYL bridges REST and histone methyltransferases for gene repression and suppression of cellular transformation. Mol. Cell *32*, 718–726.

O'Carroll, D., Scherthan, H., Peters, A.H., et al. (2000). Isolation and characterization of Suv39h2, a second histone H3 methyltransferase gene that displays testis-specific expression. Mol. Cell. Biol. *20*, 9423–9433.

Rea, S., Eisenhaber, F., O'Carroll, D., et al. (2000). Regulation of chromatin structure by site-specific histone H3 methyltransferases. Nature *406*, 593–599.

Regairaz, M., Zhang, Y.W., Fu, H., et al. (2011). Mus81-mediated DNA cleavage resolves replication forks stalled by topoisomerase I-DNA complexes. J. Cell Biol. *195*, 739–749.

Sanjana, N.E., Cong, L., Zhou, Y., et al. (2012). A transcription activator-like effector toolbox for genome engineering. Nat. Protoc. *7*, 171–192.

Sarraf, S.A., and Stancheva, I. (2004). Methyl-CpG binding protein MBD1 couples histone H3 methylation at lysine 9 by SETDB1 to DNA replication and chromatin assembly. Mol. Cell *15*, 595–605.

Schultz, D.C., Ayyanathan, K., Negorev, D., et al. (2002). SETDB1: a novel KAP-1-associated histone H3, lysine 9-specific methyltransferase that contributes to HP1-mediated silencing of euchromatic genes by KRAB zinc-finger proteins. Genes Dev. *16*, 919–932.

Shechter, D., Dormann, H.L., Allis, C.D., et al. (2007). Extraction, purification and analysis of histones. Nat. Protoc. *2*, 1445–1457.

Shibahara, K., and Stillman, B. (1999). Replication-dependent marking of DNA by PCNA facilitates CAF-1-coupled inheritance of chromatin. Cell *96*, 575–585.

Sirbu, B.M., Couch, F.B., and Cortez, D. (2012). Monitoring the spatiotemporal dynamics of proteins at replication forks and in assembled chromatin using isolation of proteins on nascent DNA. Nat. Protoc. *7*, 594–605.

Soria, G., Polo, S.E., and Almouzni, G. (2012). Prime, repair, restore: the active role of chromatin in the DNA damage response. Mol. Cell *46*, 722–734.

Stuwe, T., Hothorn, M., Lejeune, E., et al. (2008). The FACT Spt16 'peptidase' domain is a histone H3-H4 binding module. Proc. Natl Acad. Sci. USA *105*, 8884–8889.

Tachibana, M., Ueda, J., Fukuda, M., et al. (2005). Histone methyltransferases G9a and GLP form heteromeric complexes and are both crucial for methylation of euchromatin at H3-K9. Genes Dev. *19*, 815–826.

Vermeulen, M., Eberl, H.C., Matarese, F., et al. (2010). Quantitative interaction proteomics and genome-wide profiling of epigenetic histone marks and their readers. Cell *142*, 967–980.

Whitehouse, I., and Smith, D.J. (2013). Chromatin dynamics at the replication fork: there's more to life than histones. Curr. Opin. Genet. Dev. *23*, 140–146.

Xu, C., Bian, C., Yang, W., et al. (2010). Binding of different histone marks differentially regulates the activity and specificity of polycomb repressive complex 2 (PRC2). Proc. Natl Acad. Sci. USA *107*, 19266–19271.

Xu, M., Wang, W., Chen, S., et al. (2012). A model for mitotic inheritance of histone lysine methylation. EMBO Rep. *13*, 60–67.

Yang, X., Li, L., Liang, J., et al. (2013). Histone acetyltransferase 1 promotes homologous recombination in DNA repair by facilitating histone turnover. J. Biol. Chem. *288*, 18271–18282.

Yang, X., Yu, W., Shi, L., et al. (2011). HAT4, a Golgi apparatus-anchored B-type histone acetyltransferase, acetylates free histone H4 and facilitates chromatin assembly. Mol. Cell *44*, 39–50.

Zee, B.M., Britton, L.M., Wolle, D., et al. (2012). Origins and formation of histone methylation across the human cell cycle. Mol. Cell. Biol. *32*, 2503–2514.

Zhang, Y., Yang, X., Gui, B., et al. (2011). Corepressor protein CDYL functions as a molecular bridge between polycomb repressor complex 2 and repressive chromatin mark trimethylated histone lysine 27. J. Biol. Chem. *286*, 42414–42425.

Zhu, B., and Reinberg, D. (2011). Epigenetic inheritance: uncontested? Cell Res. *21*, 435–441.